Interfacial properties of square-well chains from molecular dynamics simulation

Jesús Algaba[a], Agustin Morales-Aragon[a], Cristóbal Romero-Guzmán[a], Paula Gómez-Álvarez[a] and Felipe J. Blas[a*]

[a]Laboratorio de Simulación Molecular y Química Computacional, CIQSO-Centro de Investigación en Química Sostenible and Departamento de Ciencias Integradas, Universidad de Huelva, 21007 Huelva, Spain

ARTICLE HISTORY
Compiled January 19, 2026

ABSTRACT
Square-well (SW) potential is likely the simplest potential describing attractive and repulsive interactions. However, its discontinuous functional form makes it difficult to be used in Molecular Dynamics (MD) simulation, particularly with commercial MD packages. Recently, Zerón and collaborators [*Mol. Phys.* **116**, 3355 (2018)] have presented a parameterization of the SW potential that allows its use for simulation packages since the intermolecular potential and force are described by continuous mathematical functions. It was validated for SW spheres. In this work, we use this reported continuous SW potential to describe for the first time the equilibrium and interfacial properties of SW chains, with potential ranges of $\lambda = 1.5$ and 1.75. Simulations for tetramers interacting with $\lambda = 1.5$ are compared with available computational data in the literature, which has allowed to validate the method for molecular chain systems. Besides, a systematic study for the potential range of $\lambda = 1.75$ has not been addressed so far, which represents valuable information for instance to discern whether different microscopic theories are capable of describing this type of system. In particular, we assess the effect of temperature, chain length, and potential range on the calculated properties, namely density profiles, coexistence densities, vapour pressures, surface tensions and critical points. Overall, with increasing the chain length, the width of the envelope of the coexistence phase increases, which results in an increase of the surface tension as well as the critical temperature at the same time that the vapour pressure and the interfacial width decrease.

KEYWORDS
Molecular Dynamics, interfacial properties, square-well chains, vapour-liquid phase equilibria

1. Introduction

The knowledge of interfacial properties is essential from a fundamental and industrial point of view. [1] Although it is possible to experimentally obtain phase equilibria of molecular systems with standard techniques, [2, 3] including among others coexistence densities and the surface tension, some other properties such as density profiles or interfacial thickness are very difficult to measure. In this sense, molecular simulation represents an alternative or complement to experimental studies. The increase in com-

CONTACT Felipe J. Blas. Email: felipe@uhu.es

putational power and a large number of techniques [4, 5] that have been developed in the last decades allows the characterisation of the macroscopic properties of a certain system, such as the interfacial properties of inhomogeneous fluids or mixtures, as well as its underlying microscopic behaviour.

More specifically, the phase equilibrium of molecular chains has been largely studied, experimentally and by using either theoretical models or molecular simulation. [6–31] The level of complexity in describing the molecular chain on the microscopic scale of length and time is wide ranging, from the most detailed realistic "all-atoms" and "united-atoms" models, such as TraPPE models [32] to coarse-grained models or simple molecular chain models [33]. In this latter case, fully flexible chains comprised from tangentially-bonded monomeric units are commonly adopted, which means that the bond length between consecutive bonded monomers is equal to the hard-sphere diameter of the monomer. The monomers like-that bonded and interacting through effective potentials probably represent the simplest option for preserving the basic microscopic characteristics of the molecular chains. These are basically segment connectivity, molecular flexibility, and attractive and repulsive dispersive interactions between monomers. Both attractive and repulsive interactions are accounting in a simple manner by the Square-Well (SW) potential. According to the SW intermolecular potential, two particles will only interact when their centre-to-centre distance is between σ and $\lambda\,\sigma$. Here σ denotes the diameter of the hard-sphere core of the SW particles and λ the intermolecular potential range. Hence, this model has two discontinuities, at $r = \lambda\,\sigma$ and at $r = \sigma$, which imply that the standard resolution techniques valid for continuous potentials are not suitable in this case. For the MD simulation method, this problem is even more delicate since at the discontinuities of the discrete potential the force does not exist. Discrete potentials such as SW cannot hence be used for standard codes, and special techniques are required. Recently, Orea and Odriozola [34] have proposed the so-called Constant Force Approach (CFA) to deal with discontinuous interaction potentials. The discrete nature of the interaction potential is modeled by the constant force approximation, which allows the direct calculation of the thermodynamic properties such as the pressure tensor of SW fluids. Padilla and Benavides [35] and Torres-Carbajal *et al.* [36] conducted molecular simulations using this approach to account for the liquid-vapor phase diagram and the self-diffusion coefficient, respectively, of the SW fluid for an interaction range of $\lambda = 1.5$. Also, Sandoval-Puentes *et al.* [37] and Perdomo-Pérez *et al.* [38] have implemented a soft representation of the SW potential to also examine SW monomer fluids for an interaction range of $\lambda = 1.5$ among others. Chapela and Alejandre [27] and Martínez-Ruiz *et al.* [31] conducted molecular simulations to calculate the phase equilibrium and interfacial properties of SW chains using MD and MC methods, respectively. In both cases, the SW potential was dealt taking specifically into account the discontinuities that this potential presents, and also explicitly accounting the impulsive forces generated in the system in MD simulations. Both studies were limited to SW chains with a potential range of $\lambda = 1.5\,\sigma$. It is important to note here that the model simulated by Chapela and Alejandre is not strictly a fully flexible tangent model of SW chains but a vibrating model of SW chains. In such case, the bond length is not strictly constant but exhibits a variation of $\pm 0.03\,\sigma$ around the average bond length, which is $0.97\,\sigma$ in the simulations of Chapela and Alejandre.

Recently, Zerón *et al.* [39] have presented a parameterization of the SW potential that allows its use for simulation packages such as GROMACS [40] or LAMMPS [41], since the intermolecular potential and force are mimicked by continuous mathematical functions. The continuous version of the potential (CSW) solves the above-exposed

problems. They determined the interfacial properties and the phase equilibrium of SW spheres with different ranges of interaction using GROMACS. The excellent agreement of the obtained results with available experimental data showed that the reported methodology is capable of providing confident predictions. The current work intends to extend the study conducted by Zerón *et al.* [39] by characterising the vapour-liquid (VL) phase equilibrium of molecular chains using the continuous SW potential proposed by these authors for the GROMACS package. [40] First, we perform simulations at different temperatures for chains formed from four monomers with a potential range of $\lambda = 1.5$ in order to compare with the reported computational predictions [27, 31] for this system. This comparison allows to assess the effectiveness of the SW continuous potential using GROMACS simulation package (version 4.6.1) in the case of describing molecular chains. Then, we considered molecular chain systems comprising four, eight, and sixteen monomers with a potential range of $\lambda = 1.75$. We thus analyse the effects of temperature, chain length and potential range on the calculated properties, namely density profiles, coexistence densities, vapour pressures, temperature and critical densities and surface tensions. It is worth noting that no data have been found in the literature obtained by molecular simulation of this type of system. From our knowledge, this is the first time that the phase equilibrium of SW molecular chains interacting with potential range $\lambda = 1.75$ is computed by using direct coexistence simulations. The reported information is hence valuable, for instance, to discern whether microscopic theories, such as those based on the density functional theory [42] or equations of state such as the statistical theory of associating fluids, [43, 44] based on Wertheim's theory, [45–48] are capable of characterising the VL phase equilibria of these systems.

The remainder of the paper is organised as follows: in Section 2 we include the description of the used molecular models and simulation details as well of the procedures for determining the equilibrium, interfacial and critical properties of the targeted systems. In section 3, we comprehensively expose and discuss the results. Finally, some concluding remarks are given in Section 4.

2. Methodology

Next, we present the methodology used in this work, from the molecular model describing the chains under study, to other important simulation details such as the initial configurations of the systems and the technical program parameters to assure the correct evolution. Also, since the work focuses on the study of phase equilibrium and the interfacial properties, we briefly describe the techniques used to determine density profiles, coexistence densities, vapour pressure and VL surface tension.

2.1. Molecular models

The molecular chains are modelled as usual: Completely flexible chains with fixed bond distances between adjacent monomers equal to the segment diameters. The SW potential is spherically symmetric and capable of describing both repulsive and attractive interactions between the segments that are part of different chains (intermolecular interactions) and between segments that are part of the same chain and separated by at least one other monomer (intramolecular interactions). The SW potential between two monomer units, in the same or in different molecules, is given by

$$\phi_{ij}(r_{ij}) = \begin{cases} \infty & r_{ij} \leq \sigma \\ -\epsilon & \sigma < r_{ij} \leq \lambda\sigma \\ 0 & r > \lambda\sigma \end{cases} \tag{1}$$

where r_{ij} denotes the distance between the centres of the two segments, σ is the diameter of the hard-sphere core of the segments, λ is the intermolecular potential range, and ϵ is the dispersive interaction of depth. We considered the values characterising the methane molecule: $\sigma = 0.373\,\text{nm}$, $\epsilon/k_B = 147.5\,\text{K}$, and molecular mass $m = 16\,\text{u}$. As previously commented, there is no continuity of the function describing this potential at distances of σ and $\lambda\,\sigma$, which makes unfeasible the computation of properties using commercial programs of MD such as GROMACS [40] or LAMMPS. [41] The recently reported continuous SW potential [39] solves this problem. The specific functional form of this SW interaction potential is given by, [39]

$$\phi_{ij}(r_{ij}) = \frac{1}{2}\left\{\left(\frac{1}{r_{ij}}\right)^n + \frac{1 - \mathrm{e}^{-m(r_{ij}-1)(r_{ij}-\lambda)}}{1 + \mathrm{e}^{-m(r_{ij}-1)(r_{ij}-\lambda)}} - 1\right\} \tag{2}$$

where n and m are parameters fitted to describe the softness of the repulsive and attractive parts of the intermolecular potential, respectively. According to Zerón *et al.*, [39] $n = 2500$ and $m = 20000$ allow to describe correctly the thermodynamic and interfacial properties of the SW model fluid. This optimal parametrization and other important details, such as the consequent functional form for the force between pairs of SW spheres, can be consulted in the original paper. [39]

2.2. Simulation details

MD simulations of the systems were performed using the direct coexistence technique. The assembly of the initial simulation box is the most important step and requires great effort and attention, since any error would make the system to evolve through non-stable microstates, which would imply very long computation times to reach the equilibrium at the thermodynamic conditions imposed during the simulation. The number of chains, N, that has been used in the simulations depends on the length of the chain, in the way that there is the same number of monomers for all the systems. Thus, for 2016 monomers, N is equal to 504, 252 and 126 for chain SW with $m = 4$, 8 and 16 monomers, respectively. We denote L_x, L_y, and L_z the dimension of the simulation box in the x, y, and z directions. The starting procedure of the simulation consists of placing the set of 2016 monomers in the centre of the simulation box, surrounded by vacuum on both sides, and allowing them to evolve through all the accessible microstates by calculating the interacting energy at certain temperature conditions. The initial homogeneous liquid slab is placed in a rectangular simulation box of dimensions $L_x = L_y = 11\,\sigma$, and $L_z = 24$, 26, and $28\,\sigma$ for SW chains formed from 4, 8, and 16 monomeric units, respectively. The final overall dimensions of the interfacial simulation box (vapour-liquid-vapour configuration) are $L_x = L_y = 11\,\sigma$, and $L_z = 72$, 78, and $84\,\sigma$ for the corresponding chain lengths. Periodic boundary conditions are used in the three directions of the simulation box, so that it is possible to minimise the effects of finite size of the system.

Once the initial configuration is assembled, it is necessary to define a series of variables that will ensure the proper transition from the initial molecular system to the state of thermodynamic equilibrium determined by the selected ensemble. The simulations were conducted at different temperatures in the NVT ensemble using the MD program GROMACS (version 4.6.1). [40] The temperature of the system was controlled by using the Nosé-Hoover thermostat with a coupling constant value of 2 ps. [49, 50] According to the work of Zerón *et al.* [39] we used a time step of 0.1 fs due to the complex functional forms of the interaction potential and force between segments that form the chains, especially at $r = \sigma$ and $r = \sigma\,\lambda$ where the potential slope is very steep. This time step is considerably lower than the standard values used in rigid (2 fs) and flexible (1 fs) systems that interact through the Lennard-Jones potential. However, higher values of time step in this case would not allow to adequately evaluate the values of the potential and the forces suffered by two segments, preventing an adequate exploration of the phase space of the system.

In order to obtain an adequate description of the potential and the interaction force using GROMACS software, their respective expressions, reported in Zerón *et al.*, [39] must be expressed in tabular form. In particular, the potential has been tabulated with a mesh of $\delta\,r = 0.00001\,\text{nm}$, so it has been necessary to carry out all the calculations with double precision. [40] The values of temperatures considered in this work were selected throughout the liquid range of each of the systems, from values of 50% of the critical temperature estimated from the SAFT-VR equation of state, [51, 52] up to values of 80-85% of the critical temperature of each system. This approximate information on thermodynamic conditions is valuable as starting point to conduct simulations for phase equilibria of the systems. In all the simulations, we considered 10 ns of equilibration and 50 ns of data collection. The production run was divided into 10 blocks of 5 ns. Thus, the equilibrium values of the vapour pressure and surface tension are determined as the average over the blocks, and the corresponding errors as the standard deviation over the average of the blocks.

2.3. Calculation of properties

In the following lines, we explain the procedures for the calculation of the properties characterising the phase equilibrium and the interface of the chain systems. As it is well-known, an interface appears when two phases coexist in a first-order phase transition, separating one bulk phase from the other. There is an interfacial width, d, along which the properties vary from the values taken in one bulk phase to the values taken in the other bulk phase. For example, at a VL interface, the density varies continuously from the coexisting density of liquid ρ_L to that of vapour ρ_V. For a correct calculation of both coexistence densities, a careful treatment of the density profile becomes essential. Making use of the direct coexistence simulation technique, it is possible to determine the density of the system as a function of the position along the interface $\rho(z)$ (density profiles), at different temperatures. To this end, as commented above, the simulations are conducted in the canonical ensemble, in which the volume of the system remains constant. The density profiles $\rho(z)$ are determined following the standard methodology. The z direction of the simulation box, the direction normal to which the interface develops, is divided into n_s layers (slabs) of thickness $\Delta = L_z/n_s$ parallel to the interface (xy plane). Then, the molecular density of the system is obtained by associating the molecular position to the corresponding slab, in a way that is possible to define $\rho(z)$ by averaging, once the system is balanced, the number of molecules

$N(z)$ in each layer of thickness $\Delta\, z$ centred on z, of volume $V_s = L_x\, L_y\, \Delta\, z$. The value of the slab thickness $\Delta\, z$ must be small enough to obtain a proper discretization of the system, and large enough so that the statistical precision is adequate. In this work, the z-direction of the box has been divided into $n_s = 200$ slabs. To ensure stable values of the equilibrium coexistence densities, they are obtained by averaging $\rho(z)$ over the bulk vapour and liquid zones far enough from the interfacial zone. In particular, since the system has been prepared in such a way that the liquid phase is in the centre of the box, the coexistence density is approximately obtained by averaging over the central 25% of the lateral (for the vapour phase, ρ_V) and central (for the liquid phase, ρ_L) zone of the density profiles. The statistical errors are estimated by the standard deviation of the mean values.

Other interesting properties to study are the vapour pressure and the surface tension. The vapour pressure is defined as the force per unit area exerted by a fluid on a real or imaginary surface. It is very informative about the thermodynamic state of an inhomogeneous system, since it affects its chemical equilibrium at the interfaces. The surface tension is the Gibbs energy per unit area at the interface, for certain thermodynamic conditions, and plays a crucial role in multiphase systems. Both magnitudes are determined from the pressure tensor. Although several mechanical or thermodynamic methods can be used to obtain these magnitudes, here we follow the mechanical (virial) route, [53] and particularly the Irving-Kirkwood approach. In an inhomogeneous system with flat interfaces perpendicular to the z direction, as occurs in this work, we distinguish two components of the pressure tensor, namely tangential P_T and normal P_N pressure. They are functions of the position in the fluid, in particular of the distance measured perpendicularly to the interface, z. The virial expressions used to calculate both pressure components can be found elsewhere. [42] The equilibrium vapour pressure of the system is equal to the normal pressure. The surface tension is obtained from the difference between both pressure components.

Finally, from the VL coexistence curve of a system it is possible to estimate the critical temperature T_c, and the critical density, ρ_c. To this end, we apply the well-known scaling law[54, 55] given by the following equations,

$$\rho_L - \rho_V = A\,(T - T_c)^{\beta} \tag{3}$$

$$\frac{\rho_L + \rho_V}{2} = \rho_c + B\,(T - T_c) \tag{4}$$

Here β is the corresponding critical exponent,[56] with a universal value of $\beta = 0.325$ in Eq. (3). Eq. (4) is the well-known law of rectilinear diameters. A, B, T_c and ρ_c are four unknown constants obtained by fitting to the simulation results. ρ_L and ρ_V are the liquid and vapour coexistence densities at the corresponding temperature T, respectively. Critical temperature, T_c, and density, ρ_c, can be easily obtained from Eqs. (3) and (4).

An alternative and independent way [57, 58] to estimate the critical temperature T_c is from the obtained surface tension values as a function of temperature, $\gamma(T)$, using the scaling relation given by Eq. (5)

$$\gamma = \gamma_0 \left(1 - T/T_c\right)^{\mu} \tag{5}$$

where γ_0 is the so-called "zero-temperature" surface tension and μ is the corresponding critical exponent. Here, we fix μ to the universal value of $\mu = 1.258$, as obtained from renormalisation-group theory.[56] Once again, the unknown constants, γ_0 and T_c, are found by fitting the surface tension data with temperature. It is worth remarking that Eqs. (3)-(5) are not exact (other than at temperatures very close to the critical point), and additional terms should be required for a highly accurate determination of the density and surface tension.

The critical pressure can be estimated from an extrapolation of the Clausius–Clapeyron relation to the critical temperature obtained from Eqs. (3) or (5):

$$\ln P = C_1 + \frac{C_2}{T} \tag{6}$$

where C_1 and C_2 are correlation parameters. The value of the critical pressure, P_c, is obtained using Eq. (6) at $T = T_c$. The critical temperature value used in the previous equation is obtained from Eq. (3).

All the quantities in our paper are expressed in conventional reduced units, with σ and ϵ being the length and energy units, respectively. Thus, the temperature is given in units of ϵ/k_B, the densities in units of σ^{-3}, the lengths, including the interfacial thickness, in units of σ, the pressures in units of ϵ/σ^3, and the surface tension in units of ϵ/σ^2.

3. Results

Since the SW molecular chains comprised by four monomers with potential range $\lambda = 1.5$ has been studied by Chapela and Alejandre [27] and Martínez-Ruiz *et al.*, [31] using MD and MC methods, respectively, we first discuss the results of equilibrium phase and interfacial properties obtained for this system. The comparison will allow to assess the reliability of the implementation of the continuous form of the SW potential and its use for molecular chains, as well as of the overall methodology used in this work. Then, it is applied to obtain information for a potential range not previously studied ($\lambda = 1.75$). Table 1 summarises the results at different temperatures for this system of the coexistence densities, the vapour pressure, and the surface tension, obtained as previously explained in methodology section. The errors of vapour pressure and surface tension are estimated according to the explanation included in the previous section. In the case of liquid and vapour densities, we use the values of the equilibrium density profile corresponding to the liquid and vapour regions, respectively. For the interfacial thickness, we use only one of the two values obtained from the fitting of the density profiles (see the next paragraph).

Once the liquid and vapour densities, ρ_L and ρ_V, at each temperature are determined, by averaging the proper regions of the density profiles, each density profile is adjusted to the hyperbolic tangent function given by,

Table 1. Liquid density, ρ_L, vapour density, ρ_V, vapour pressure, P, interfacial width, d, and surface tension, γ, at different temperatures for systems of fully flexible CSW chains formed from four monomers with potential range $\lambda = 1.5$. The estimated errors are estimated as explained in the text. Nomenclature means the following: $0.801(4) = 0.801 \pm 0.004$.

T	ρ_L	ρ_V	P	d	γ
1.00	0.801(4)	0.000002(12)	0.00009(9)	0.7534	0.77(2)
1.20	0.752(3)	0.000184(3)	0.0002(4)	1.0080	0.58(1)
1.30	0.724(3)	0.000689(5)	0.00051(8)	1.2574	0.48(1)
1.40	0.693(3)	0.00203(3)	0.00143(5)	2.5845	0.380(9)
1.50	0.655(2)	0.0097(3)	0.00314(6)	2.2413	0.29(1)
1.60	0.609(2)	0.0222(8)	0.0068(1)	2.3029	0.178(9)
1.65	0.581(2)	0.0320(9)	0.0092(1)	3.0509	0.139(7)

Table 2. AAD% of the simulation results for fully flexible CSW chains formed from four monomers with potential range $\lambda = 1.5$ with respect the simulation data for the liquid (ρ_L) and vapour (ρ_V) densities, interfacial tension (γ) and critical temperature (T_c) and density (ρ_c) obtained for the same system by Chapela and Alejandre [27] and Martínez-Ruiz *et al.*, [31]. Critical temperature (T_c) and density (ρ_c) reported in this work for the fully flexible CSW chains are calculated from Eq. (3) and Eq. (4).

	AAD%(ρ_L)	AAD%(ρ_V)	AAD%(γ)	AD%(T_c)	AD%(ρ_c)
Chapela and Alejandre [27]	0.24	28.09	4.56	5.80	3.84
Martínez-Ruiz *et al.* [31]	0.28	39.05	29.52	1.81	0.61

$$\rho(z) = \frac{1}{2}(\rho_L + \rho_V) - \frac{1}{2}(\rho_L - \rho_V)\tanh\left(\frac{z - z_0}{d}\right) \tag{7}$$

where z_0 and d denote the Gibbs dividing surface and the interfacial width of each interface, respectively. This latter parameter is likewise presented in Table 1. Along all the work, only density profiles associated with one of the interfaces are dealt, in order to avoid redundant information. Likewise, in order to show all the profiles with respect to the same reference system, they have been displaced along the z axis to place the Gibbs dividing surface, z_0, at the origin of coordinates.

Fig. 1 shows the equilibrium density profiles of SW molecular chains formed from four monomers, with potential range $\lambda = 1.5$, at the temperatures exposed in Table 1. Obviously, the liquid and vapour phases correspond to the left and right sides of the interface, respectively. As it can be seen, the density of the liquid decreases and the density of the vapour increases as the temperature of the system is raised, as expected. Also, the slope of the density profiles along the interfacial region becomes smaller, in absolute value, as the temperature approaches its critical value. According to the scaling laws valid in the vicinity of the critical point, the interfacial width must diverge. The obtained results are consistent with such tendency. The critical temperature and density values obtained in this work, from Eqs. (3) and (4), are T_c=1.94(2) and ρ_c=0.27(3), respectively.

From the obtained coexistence equilibrium densities of the liquid and vapour phases at each temperature and the critical coordinates, according to procedures exposed in Section 2, we depict in Fig. 2 the VL coexistence diagram of the system, together with the respective data reported by Chapela and Alejandre [27] and Martínez-Ruiz *et al.* [31] The agreement among the simulation results of both authors and the results obtained using the continuous version of the SW intermolecular potential is excellent

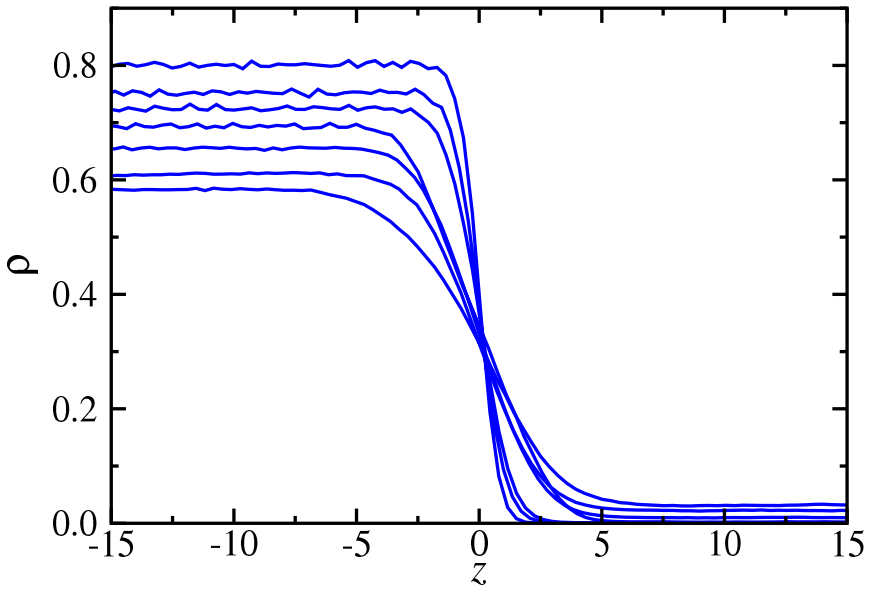

Figure 1. Simulated equilibrium density profiles across the vapour-liquid interface of fully flexible SW chains formed from four monomers with potential range $\lambda = 1.5$. From top to bottom (in liquid region): $T = 1.0$, 1.2, 1.3, 1.4, 1.5, 1.6, and 1.65.

throughout the temperature range despite using different methodologies. It is observed, however, that the estimates of the critical temperature and density slightly differ. In particular, the critical temperature obtained in this work is above the other simulation results available in the literature, especially in relation to the value reported by Chapela and Alejandre [27]. The critical temperature is obtained using the scaling law from a truncated Wegner expansion given by Eq. (3). Note that, strictly speaking, this Wegner expansion is only valid at temperatures very close to the critical temperature ($T \to T_c$). In our case, we use values between 0.5 and 0.85 times T_c. This is a large temperature distance but it is routinely used in the literature. Particularly, our highest temperature considered in the fitting is $T = 1.65$. There are two important differences with the case of Chapela and Alejandre: (1) they use an augmented Wegner expansion (see Eq. (6) of their work), and more importantly, (2) the highest temperature considered by Chapela and Alejandre is $T = 1.8$. This temperature is closer to T_c than our highest value (1.65), which contributes definitively to predict a higher value of T_c

The obtained surface tension values as a function of the temperature, collected in Table 1, are depicted in Fig. 3. The results reported by Chapela and Alejandre [27] and Martínez-Ruiz *et al.* [31] have been also included for comparison. As it can be seen, the dependence of this magnitude with the temperature is the expected: high values at low temperatures, indicating a significant separation between the liquid and vapour phases, and a tendency to decrease asymptotically to zero as the temperature of the system approaches the critical temperature. As in the case of the phase diagram, the well-known scaling relationship with the temperature in the vicinity of the critical point has been used. Although the surface tension is especially sensitive to molecular

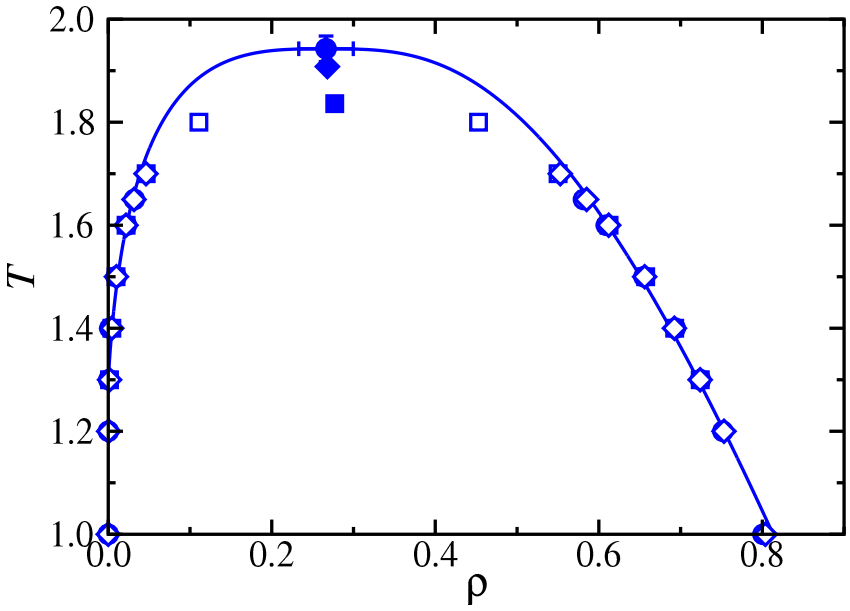

Figure 2. Vapour-liquid coexistence densities for fully flexible CSW chains formed from four monomers with potential range $\lambda = 1.5$. The circles correspond to the coexistence densities obtained from the analysis of the density profiles obtained from MD NVT simulations and the squares and diamonds correspond to the results obtained for the same system by Chapela and Alejandre [27] and Martínez-Ruiz *et al.*, [31] respectively. The filled symbols denote critical points, which were estimated in this work and in Martínez-Ruiz *et al.*, [31] from Eqs. (3) and (4), and slightly differently in Chapela and Alejandre [27]. The curve represents the fit of the simulation data obtained in this work to Eq. (4).

details, the results obtained in this work are in excellent quantitative agreement with those obtained by Chapela and Alejandre [27] throughout the temperature range considered. Unfortunately, there are important discrepancies at low temperatures when comparing with the data taken from the work of Martínez-Ruiz *et al.*, [31] who used MC methodology. This may be due to an inadequate MC exploration of the internal degrees of freedom of the molecules at low temperatures in determining the surface tension by thermodynamic methods. It is worth also comparing with computational results for SW spheres of the same range $\lambda = 1.5$ obtained by the CFA approach [34, 35]: at the reduced temperature of unity, the only comparable value, surface tension takes logical lower values than SW chains: it is in between 0.25 and 0.3.

Table 2 includes the percentage Average Absolute Deviation AAD% of our results for the liquid and vapour densities and interfacial tension at the different temperatures with respect to the data from Chapela and Alejandre [27] and Martínez-Ruiz *et al.*, [31], which is defined as:

$$\mathrm{AAD}\% = \frac{1}{N_p}\sum_{i=1}^{N_p}\left|\frac{X_i^{\mathrm{CSW}} - X_i^{\mathrm{lit}}}{X_i^{\mathrm{lit}}}\right| \times 100 \tag{8}$$

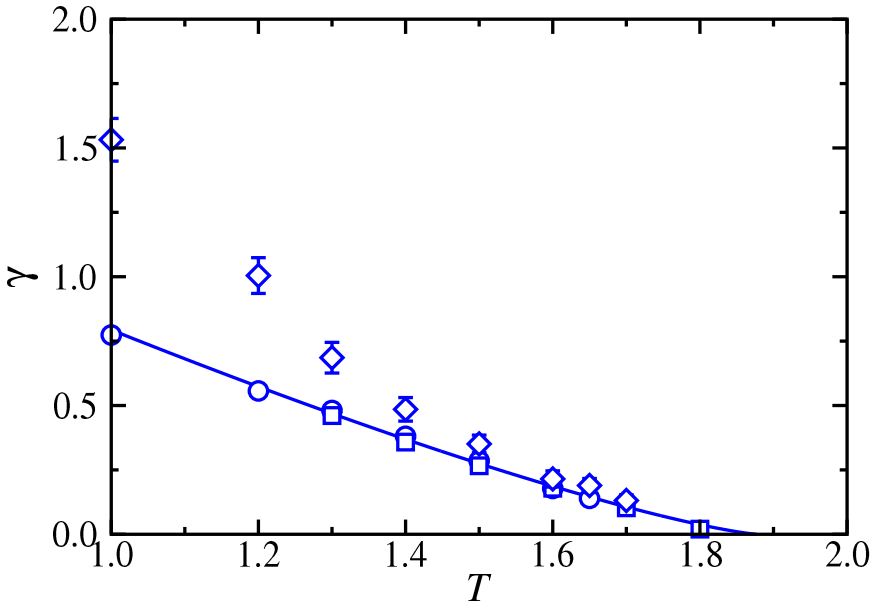

Figure 3. Surface tension, as a function of temperature, for fully flexible CSW chains formed from four monomers with potential range $\lambda = 1.5$. The symbols are the same as in Fig. 2. The curve represents the fit of our simulation data to the scaling relationship of the surface tension near the critical point given Eq. (5) with $\mu = 1.258$.

where $X_i^{\rm CSW}$ and $X_i^{\rm lit}$ denote our simulated and previously reported data, respectively, for each property; and N_p denotes the number of points, *i.e.*, of considered temperatures. This provides a quantitative and average measure of the comparison between the results obtained by the distinct methods for this SW system. We also collect in Table 2 the deviations of our critical values, $T_c = 1.94(2)$ and $\rho_c = 0.27(3)$, with respect to literature [27, 31].

Once the methodology has been demonstrated, by comparison with available data, [27, 31] capable of confidently predicting the density profiles, the VL equilibrium and the surface tension, we calculate these properties for SW chains formed from different numbers of monomers, $m = 4$, 8 and 16 with potential range $\lambda = 1.75$, at different temperatures. To our knowledge, this study has not been carried out so far, and it is necessary and interesting from various fundamental aspects. First, new simulation data for this kind of system is useful to validate molecular theories; and secondly, this allows to assess the effect of the SW potential interaction range on the interfacial properties of the systems. Figure 4 shows the density profiles of each of the chain lengths studied, as a function of the temperature. As expected, the qualitative behaviour is the same for each system and the same to that obtained for chains with potential range $\lambda = 1.5$. As the temperature increases, the density of the liquid (vapour) phase decreases (increases), and the interfacial width increases. It can be seen that, at the same temperature, the slope of the density profile, in absolute value, increases with increasing the chain length. This phenomenon can be better understood from the next results for coexistence diagrams, interfacial widths and surface tensions as a function

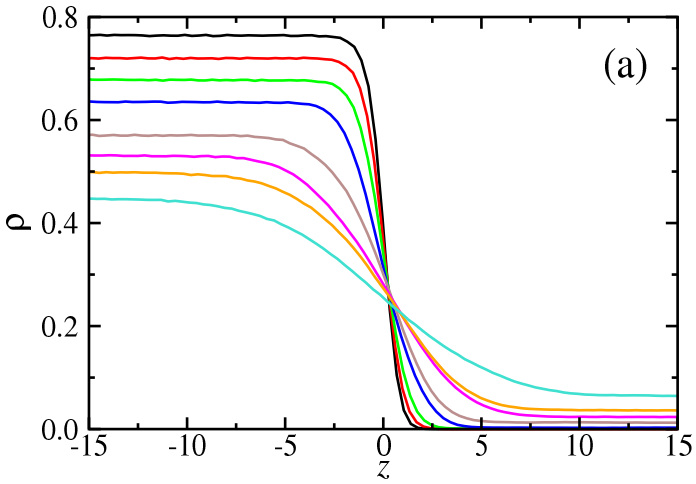

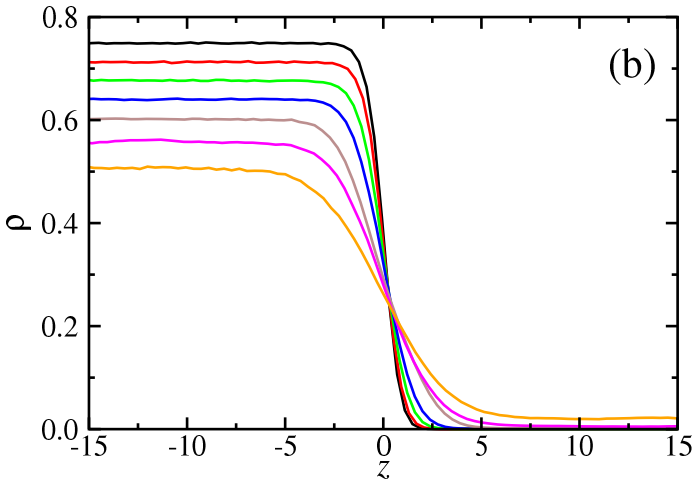

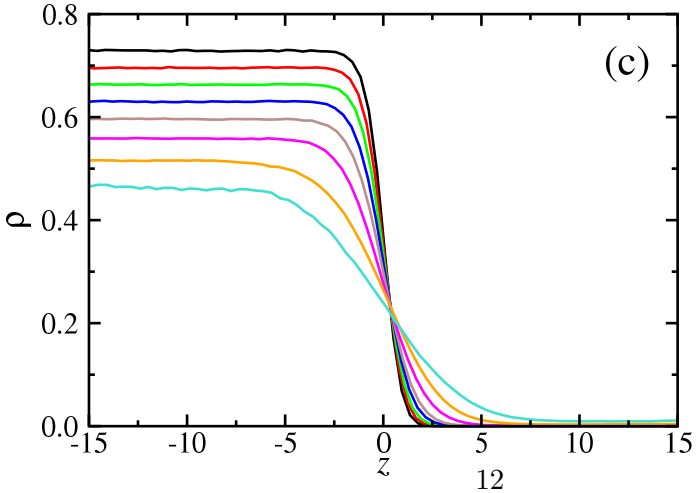

Figure 4. Simulated equilibrium density profiles across the vapour-liquid interface of fully flexible SW chains formed from four ($m = 4$), eight ($m = 8$), and sixteen ($m = 16$) monomers with potential range $\lambda = 1.75$. From top to bottom (in liquid region): (a) $m = 4$, $T = 1.45$, 1.70, 1.95, 2.20, 2.45, 2.70, 2.83, and 2.9; (b) $m = 8$, $T = 1.70$, 1.95, 2.20, 2.45, 2.70, 2.95, and 3.20; (c) $m = 16$, $T = 1.95$, 2.20, 2.45, 2.70, 2.95, 3.20, 3.45, and 3.7.

of temperature and chain length.

As previously exposed, and following the procedure described for the first system studied, the coexistence densities are obtained by averaging the proper regions of the density profiles. Then, the interfacial width is determined from the fit of the density profiles, at each temperature, to a function of hyperbolic tangent type according to Eq. (7). The vapour pressure and the surface tension are calculated from the components of the pressure tensor. Results of all these magnitudes are reported in Table 3, as a function of the temperature and chain length. In turn, from the coexistence densities, the critical magnitudes are calculated from the scaling law associated with the critical exponent β and the law of rectilinear diameters, as exposed in section 2. The critical temperatures are likewise obtained from the surface tension according to Eq. (5). The obtained values characterising the critical point are reported in Table 4. The results summarised in Tables 3 and 4 are plotted and comprehensively discussed in the following lines. Note that the vapour pressure of the longest chainlike molecule considered in this work, $m = 16$, could not be obtained at low temperatures ($T \leq 2.70$) since the number of molecules in the vapour phase was very low. It is important to mention that the direct coexistence technique is not the most appropriate method to determine vapour pressures. [59]

Table 3. Liquid density, ρ_L, vapour density, ρ_V, vapour pressure, P, interfacial width, d, and surface tension, γ, at different temperatures for systems of fully flexible CSW chains formed from four, eight, and sixteen monomers with potential range $\lambda = 1.75$. The estimated errors are estimated as explained in the text.

T	ρ_L	ρ_V	P	d	γ
		$m = 4$			
1.45	0.7644(8)	0.000003(1)	0.000002(8)	0.761(6)	1.30(1)
1.70	0.7199(8)	0.000119(4)	0.00005(1)	0.957(2)	1.056(4)
1.95	0.6778(7)	0.00074(3)	0.00032(2)	1.236(9)	0.852(8)
2.20	0.6348(8)	0.00269(8)	0.00153(4)	1.84(1)	0.647(8)
2.45	0.5703(7)	0.0126(3)	0.0068(1)	2.4(1)	0.380(8)
2.70	0.531(1)	0.02396(3)	0.0122(1)	3.6(2)	0.261(5)
2.83	0.497(1)	0.03625(3)	0.0190(2)	3.97(4)	0.175(5)
2.95	0.450(2)	0.061(1)	0.0281(1)	5.4(3)	0.101(8)
		$m = 8$			
1.70	0.7492(8)	0.0000002(8)	0.000003(4)	0.804(4)	1.244(8)
1.95	0.7124(8)	0.0000003(14)	0.000004(5)	0.917(2)	1.05(1)
2.20	0.6768(8)	0.000080(4)	0.000015(8)	1.16(1)	0.87(1)
2.45	0.6403(8)	0.00061(9)	0.00009(1)	1.50(1)	0.694(6)
2.70	0.6019(6)	0.00144(8)	0.00058(2)	2.17(3)	0.533(7)
2.95	0.560(2)	0.0059(4)	0.00176(5)	2.44(2)	0.382(6)
3.20	0.5084(20)	0.019(1)	0.0050(1)	3.2(1)	0.238(6)
		$m = 16$			
1.95	0.7289(9)	0.0000001(4)	-	0.869(5)	1.17(1)
2.20	0.6957(6)	0.0000002(8)	-	0.9812(3)	0.98(1)
2.45	0.6634(6)	0.0000001(4)	-	1.10(1)	0.84(1)
2.70	0.6303(8)	0.000014(2)	-	1.31(1)	0.68(1)
2.95	0.5960(6)	0.00019(1)	0.00002(2)	1.534(2)	0.54(1)
3.20	0.5581(9)	0.00063(2)	0.00014(3)	2.02(2)	0.42(2)
3.45	0.517(1)	0.0035(2)	0.00072(5)	2.81(4)	0.28(9)
3.70	0.464(3)	0.012(1)	0.00217(8)	3.5(2)	0.185(6)

In Figure 5 we depict the phase diagrams of the SW chains formed from 4, 8 and 16 segments that interact with potential range $\lambda = 1.75$, including the estimates of the critical points. As can be seen, the usual VL coexistence diagram of linear chains with varying the chain length is obtained. At a given temperature, there is an increase in liquid density and a decrease in vapour density with increasing the chain length, m. This behaviour is expected, since the increase of the chain length produces

Table 4. Critical temperatures and densities for systems of fully flexible CSW chains formed from m monomers with potential range $\lambda = 1.75$. Critical temperatures, $T_c^{\dagger}$ and $T_c^{\S}$, are obtained from the analysis of the MD NVT coexistence densities using Eqs. (3) and (4), and the analysis of the MD NVT surface tension data using Eq. (5), respectively. Critical densities, $\rho_c^{\dagger}$, are also obtained from the analysis of the MD NVT coexistence densities using Eq. (4).

m	$T_c^{\dagger}$	$T_c^{\S}$	$\rho_c^{\dagger}$
4	3.17(1)	3.17(2)	0.234(5)
8	3.75(2)	3.75(4)	0.225(8)
16	4.22(2)	4.21(6)	0.210(7)

an increase in the attractive interactions in the system, which results in an increase in the separation, in terms of density, between the involved phases. This behaviour occurs at each targeted temperature, which produces a global displacement of the VL coexistence curves towards higher temperatures. Hence, the critical temperature of SW molecular chains increases with increasing the length, as a consequence of the increase in attractive interactions in the system. In short, coexistence curves become wider as the chain length increases. Also, it is interesting to comment on another more subtle effect, which has already been reported. [60, 61] as the chain length increases, the behaviour of the coexistence diagrams tends asymptotically towards that of a system made up of infinitely long chains. In particular, it is observed that the increase in width of the coexistence curve is more significant when the number of segments increases from four to eight than when the chain length increases much more. This also occurs for the critical properties, which is actually consistent with the well-known asymptotic behaviour of VL coexistence curves of molecular chains as the chain length increases indefinitely.

As it is apparent from Table 3, a few values of the vapour pressure at low temperatures ($m = 16$) are not presented (see dashed lines). The results obtained from the MD NVT simulations gave negative values for these states. According to Vega *et al.*[62] and Feria and coworkers [59] this is due to the fact that the direct coexistence technique is not appropriate to determine the vapour pressure of this type of system, especially at low temperatures, due to the extremely low values that the vapour pressure takes. Instead of this technique, it would be desirable to use the Gibbs ensemble method or free energy calculations, which will allow determining the vapour pressure more accurately for such conditions. Except for these values, the vapour pressure is depicted as a function of the temperature for SW molecular chains with different chain lengths in Fig. 6. For a given chain length, the vapour pressure of the system increases as the temperature increases, as expected. These curves follow the Clausius law, so the greater the change in pressure with temperature is, the steeper the curve is. Regarding the effect of the chain length: at a given temperature, the smaller the number of chain monomers is, the steeper the curve is. This is due to the lower intermolecular interactions in shorter systems, which implies greater volatility. As the chain length increases, the critical temperature of these systems increases, and hence the vapour pressure curves shift toward lower pressures and higher temperatures. This behaviour is consistent with computational results using the CFA approach reported by Orea

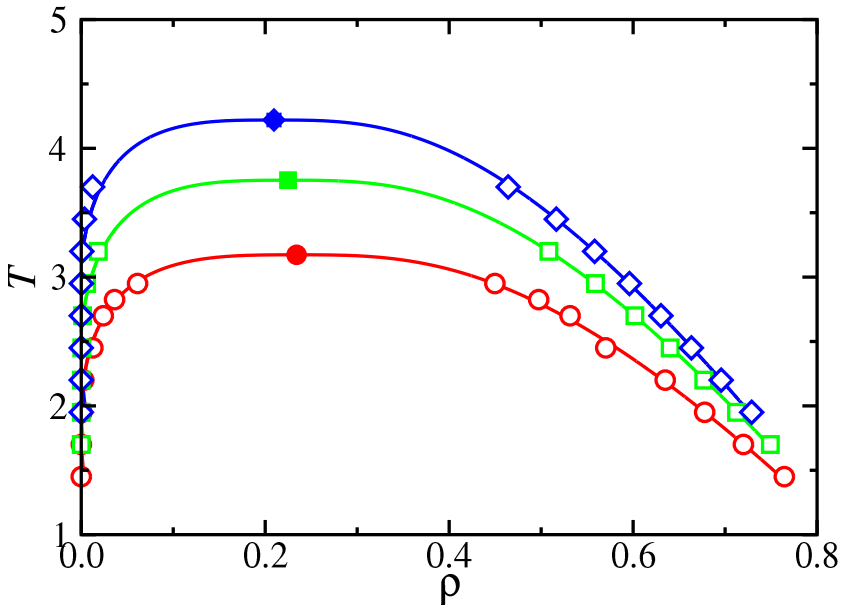

Figure 5. Vapour-liquid coexistence densities for fully flexible CSW chains with potential range $\lambda = 1.75$. The open red circles, green squares, and blue diamonds correspond to the coexistence densities obtained from the analysis of the density profiles obtained from MD NVT simulations for chain lengths of $m = 4$, 8, and 16, respectively. The filled symbols are the corresponding critical points estimated from Eqs. (3) and (4), and the curves represent the fits of the simulation data to Eq. (4).

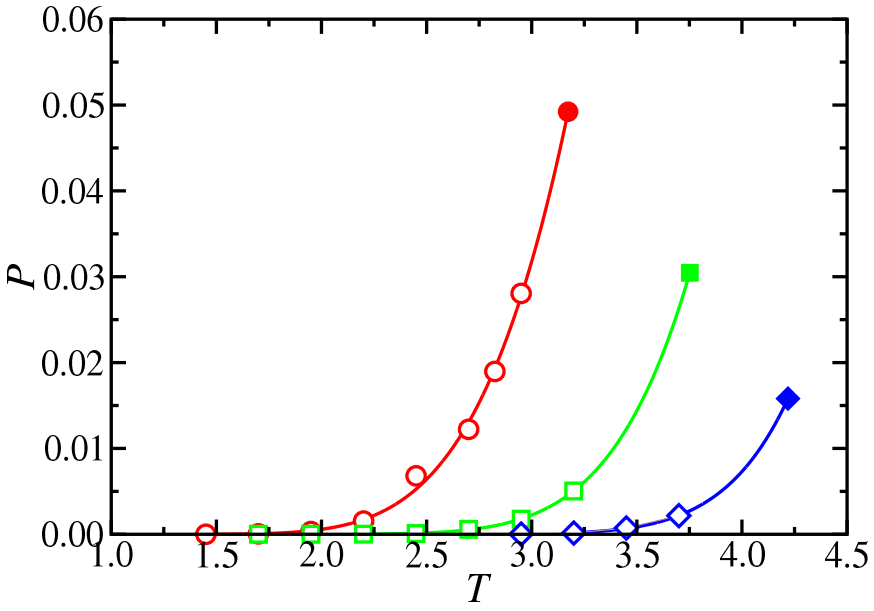

Figure 6. Vapour pressure for fully flexible CSW chains with potential range $\lambda = 1.75$. The open red circles, green squares, and blue diamonds correspond to the vapour pressure obtained from MD NVT simulations for chain lengths of $m = 4$, 8, and 16, respectively. The filled symbols are the corresponding critical points calculated from Eq. (6) evaluated at the critical temperature estimated from Eq. (3). The curves represent the fits of the simulation data to Eq. (6).

and Odriozola [34] and Padilla and Benavides [35] for SW spheres, of a range $\lambda = 1.5$.

We have also represented the vapour pressure simulation data in a Clausius–Clapeyron plot in Fig. 7. We have discarded the pressure values obtained from simulation at low temperatures due to the reasons explained in the previous paragraph. According to this, we fit the vapour pressure values represented in the figure to the Clausius equation given by Eq. (6) for all the SW chains studied in this work. As can be seen, the vapour pressure data using this representation show a linear behaviour in agreement with Eq. (6). This result corroborates that vapour pressure obtained at high temperatures, as indicated in the previous paragraph, can be obtained from the direct coexistence technique with confidence.

The reported values (see Table 3) of the interfacial width d, obtained from analysis of the density profiles, are plotted as a function of temperature for the different molecular systems in Fig. 8. On the one hand, for a given chain size, the interfacial width increases as the temperature increases. This behaviour is compatible with the shape change of the density profiles with the temperature at the VL interface. As the temperature increases, the profiles flatten in the interfacial region, as can be seen in Fig. 4, increasing hence the interfacial width. When the temperature of the system approaches the critical temperature, the interfacial width diverges (which means a flat density profile), since both phases, vapour and liquid, become one in the critical state. On the other hand, for a given temperature, the interfacial width is observed to decrease with increasing the chain length. This result is compatible with those shown for

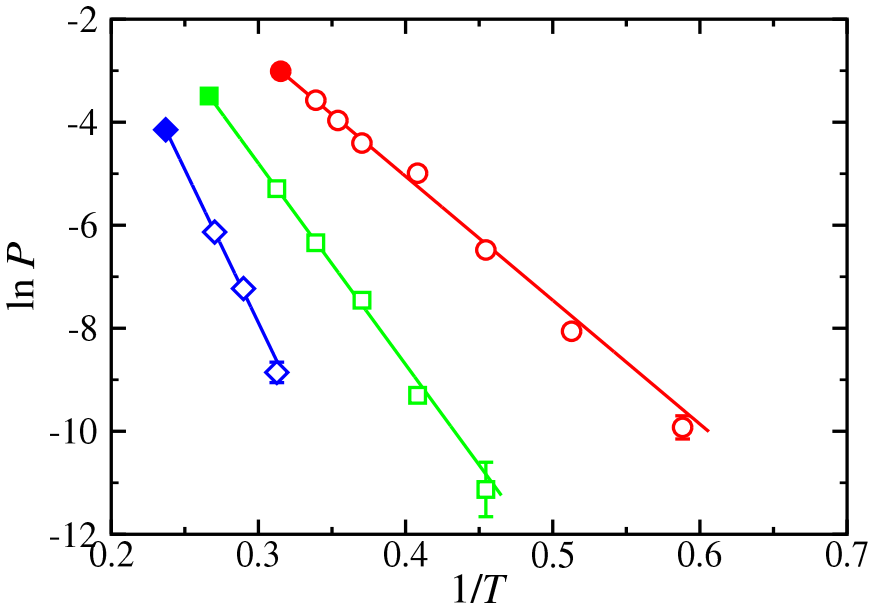

Figure 7. Clausius-Clapeyron plot for fully flexible CSW chains with potential range $\lambda = 1.75$. The meaning of the symbols and curves is the same as in Fig. 6.

the density profiles and the coexistence diagrams of chains of different lengths shown in Figs. 4 and 5, respectively. As the chain length increases, the difference between the density in the liquid phase and the gas phase increases, so the jump in densities increases. This increase corresponds to an increase in the slope, in absolute value, of the corresponding density profile in the interfacial region, with a consequent decrease in the interfacial width, as Fig. 8 evidences.

The most important interfacial magnitude is surely the surface tension, which has been determined from the mechanical route, as previously commented. Fig. 9 shows the surface tension as a function of the temperature for SW chains formed from 4, 8 and 16 monomers with potential range $\lambda = 1.75$. At a certain temperature, the surface tension increases when the chain length increases. This fact, as in the case of other thermodynamic and structural properties discussed above, is consistent with the increase of the cohesive energy of the system (attractive intermolecular interactions) as the chain length increases. The behaviour of this magnitude with the temperature is practically linear at low and intermediate temperatures, showing a slightly concave curvature in the vicinity of the critical temperature of each system. The effect of the chain length on the slope of the curve is interesting. As the molecular size increases, the slope becomes less negative and, as in the case of the coexistence curves and vapour pressures, an asymptotic behaviour is observed. These phenomena have already been described by Blas *et al.* [61] for the case of fully flexible molecular chains that interact through the Lennard-Jones potential, as well as in experimental findings for a series of homologous chains. [63] It is worth commenting that, as it is apparent from data in Table 4, the critical temperature values obtained from the surface tension are

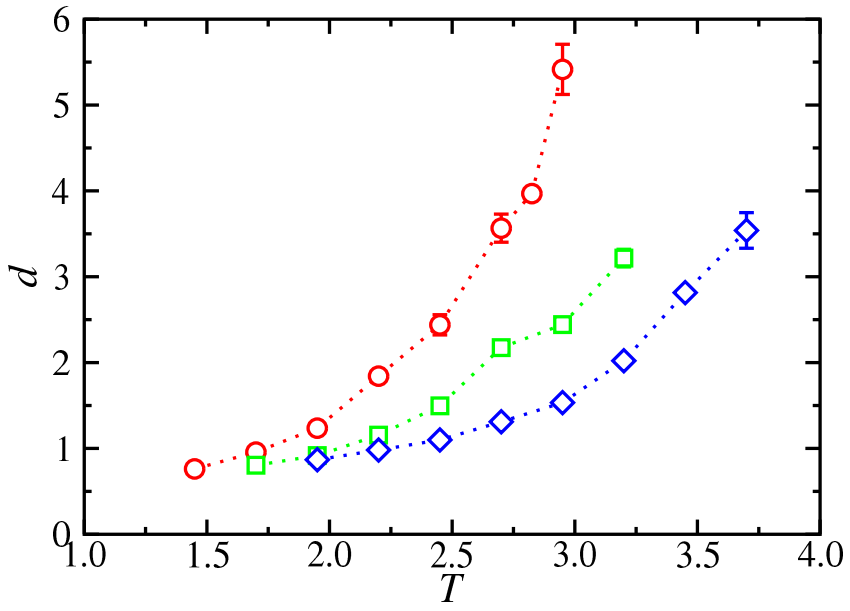

Figure 8. Interfacial thickness as a function of the temperature for fully flexible CSW chains with potential range $\lambda = 1.75$. The meaning of the symbols is the same as in Fig. 5. The curves are included as a guide to the eyes.

very similar to those obtained through the scaling relationships associated with the coexistence curves. These results corroborate our estimates of the critical temperatures of fully flexible SW chains obtained from MD NVT computer simulations. Finally, the comparison of data in Tables 1 and 3 for the chain system of $m = 4$ monomers and at similar temperature evidences that the effect of the potential range is non-negligible at all. To gain insight into this aspect, we are currently working on the phase equilibrium and interfacial properties of SW chains with $\lambda = 2.0$.

4. Conclusions

The VL phase equilibria and interfacial properties of fully flexible tangentially bonded SW chains have been determined using a recently reported continuous SW potential model by Zerón and collaborators. [39] This is the first time that molecular chain systems are studied using MD simulations with such potential, which was validated for SW spheres. We examine chains formed from four monomers with potential range $\lambda = 1.5$, and from 4, 8, and 16 monomers with potential range $\lambda = 1.75$.

The comparison and good agreement of the phase equilibria and interfacial properties of SW tetramers with potential range $\lambda = 1.5$ with available data in the literature points to the reliability of this methodology for chain systems. Then, the equilibrium and interfacial properties of SW chain fluids of 4, 8, and 16 monomeric units at different temperatures are determined for the potential range $\lambda = 1.75$. The overall behaviour

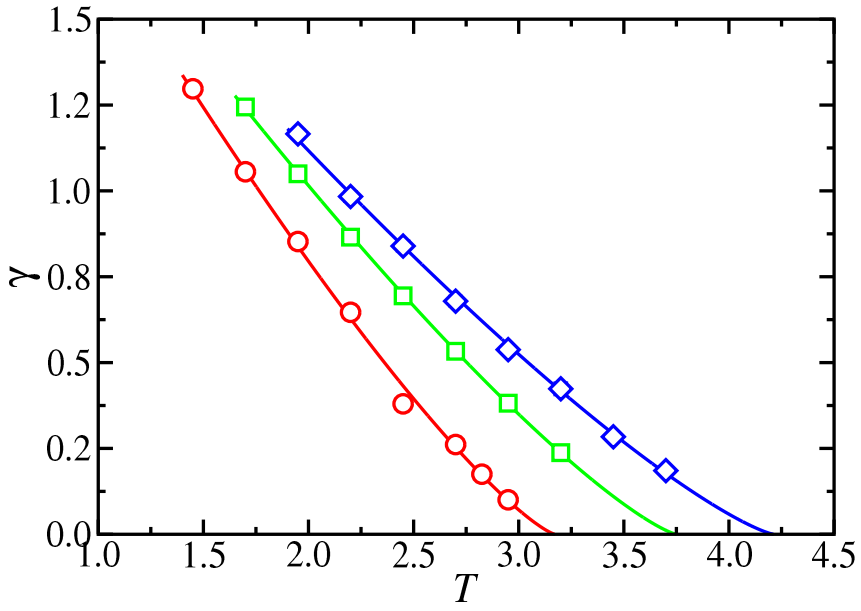

Figure 9. Surface tension as a function of the temperature for fully flexible CSW chains with potential range $\lambda = 1.75$. The open red circles, green squares, and blue diamonds correspond to the surface tension obtained from MD NVT simulations for chain lengths of $m = 4$, 8, and 16, respectively. The curves represent the fits of the simulation data to the scaling relationship of the surface tension near the critical point given Eq. (5) with $\mu = 1.258$.

of the calculated properties as a function of the temperature and of the chain length is the expected. For a given chain system, the vapour pressure and interfacial width increase as the temperature is raised, and the surface tension decreases. The contrary occurs for each property with increasing the chain length for a certain temperature. Additionally, as the chain increases, we found that the coexistence curves and the curves of surface tension with temperature exhibit an asymptotic behaviour. The estimates of the critical temperature for each system from both the coexistence densities and the surface tension are in good agreement. Clearly, the reported data evidence that the SW potential range considerably affects the thermodynamic and interfacial behaviour of chainlike systems and a more systematic study of SW chains comprising longer potential ranges is needed. This will be the subject of future work.

Finally, it is relevant to remark again that simulation results obtained in this work provide new data for SW chains useful to check if other theoretical and sophisticated tools from Statistical Mechanics are able to predict with confidence the interfacial behaviour of molecular chains with increasing potential range. This includes density functional theories, the Square Gradient Theory or other equations of state, such as the Statistical Associating Fluid Theory. This is an important issue that has not been already solved satisfactorily in the literature.

Acknowledgement

The authors thank the Centro de Supercomputación de Galicia (CESGA, Santiago de Compostela, Spain) for providing access to computing facilities.

Disclosure statement

No potential conflict of interest was reported by the authors.

Funding

This work was financed by Spanish Ministerio de Ciencia e Innovación (Grant No. PID2021-125081NB-I00), Junta de Andalucía (Grant No. P20-00363), and Universidad de Huelva (P.O. FEDER - UHU - 1255522 and FEDER - UHU - 202034), all four co-financed by EU FEDER funds, and Universidad de Huelva.

References

[1] R. Evans, *Density Functionals in the Theory of Nonuniform Fluids. In Fundamentals of Inhomogeneous Fluids* (Dekker, New York, 1992).
[2] A.W. Adamson and A.P. Gast, *Physical Chemistry of Surfaces* (John Wiley and Sons, Inc., New York, 1997).
[3] M.J.B. Evans, in *Measurement of the Thermodynamic Properties of Multiple Phases*, edited by R. D. Weir and Th. W. de Loos (Experimental Thermodynamics, Elsevier, Amsterdam, 2005), Vol. VII, Chap. 15, Measurement of Surface and Interfacial Tension, pp. 382–407.
[4] D. Frenkel and B. Smit, *Understanding Molecular Simulations* (2nd Ed. Academic, San Diego, 2002).
[5] M.P. Allen and D.J. Tildesley, *Computer Simulation of Liquids, 2 Ed.* (Oxford University Press, Oxford, 2017).
[6] V.K. Shen, R.D. Mountain and J.R. Errington, J. Phys. Chem. B **111**, 6198–6207 (2007).
[7] V.K. Shen and J.R. Errington, J. Chem. Phys. **124**, 024721/1–9 (2006).
[8] V.K. Shen and J.R. Errington, J. Chem. Phys. **122**, 064508/1–17 (2005).
[9] G.J. Gloor, G. Jackson, F.J. Blas and E.D. Miguel, J. Chem. Phys. **123**, 134703/1–19 (2005).
[10] A. Trokhymchuk and J. Alejandre, J. Chem. Phys. **111**, 8510–8523 (1999).
[11] J. Janeček, J. Phys. Chem. B **110**, 6264–6269 (2006).
[12] J.R. Errington and D.A. Kofke, J. Chem. Phys. **127** (17), 174709/1–12 (2007).
[13] E. Día-Herrera, J. Alejandre, G. Ramírez-Santiago and F. Forstmann, J. Chem. Phys. **110**, 8084/1–8 (1999).
[14] E. Díaz-Herrera, G. Ramírez-Santiago and J.A. Moreno-Razo, Phys. Rev. E **68**, 061204/1–8 (2003).
[15] E. Díaz-Herrera, J.A. Moreno-Razo and G. Ramírez-Santiago, Phys. Rev. E **70**, 051601/1–8 (2004).
[16] E. Díaz-Herrera, G. Ramírez-Santiago and J.A. Moreno-Razo, J. Chem. Phys. **123**, 184507/1–9 (2005).
[17] G. Galliero, M.M. Piñeiro, B. Mendiboure, C. Miqueu, T. Lafitte and D. Bessieres, J. Chem. Phys. **130**, 104704/1–10 (2009).
[18] P. Orea, Y. Reyes-Mercado and Y. Duda, Phys. Lett. A **372**, 7024–7027 (2008).

[19] Y. Duda, a Romero-Martínez and P. Orea, J. Chem. Phys. **126**, 224510/1–4 (2007).
[20] J.K. Singh, D.A. Kofke and J.R. Errington, J. Chem. Phys. **119**, 3405–3412 (2003).
[21] J.K. Singh and S.K. Kwak, J. Chem. Phys. **126**, 024702/1–8 (2007).
[22] J.K. Singh, G. Sarma and S.K. Kwak, J. Chem. Phys. **128**, 044708/1–8 (2008).
[23] G. Odriozola, M. Bárcenas and P. Orea, J. Chem. Phys. **134**, 154702/1–5 (2011).
[24] M. González-Melchor, G. Hernández-Cocoletzi, J. López-Lemus, A. Ortega-Rodríguez and P. Orea, J. Chem. Phys. **136**, 154702/1–6 (2012).
[25] U.F. Galicia-Pimentel, J. López-Lemus and P. Orea, Fluid Phase Equil. **265**, 205–208 (2008).
[26] E.D. Miguel, J. Phys. Chem. B **112**, 4674–4679 (2008).
[27] G.A. Chapela and J. Alejandre, J. Chem. Phys. **135**, 084126/1–11 (2011).
[28] G.A. Chapela, E. Día-Herrera, J.C. Armas-Pérez and J. Quintana-H, J. Chem. Phys. **138**, 224509/1–9 (2013).
[29] G. Jimenez-Serratos, C. Vega and A. Gil-Villegas, J. Chem. Phys. **137**, 204104/1–12 (2012).
[30] H. Peng, A.V. Nguyen and G. Birkett, Mol. Simul. **39**, 129–136 (2013).
[31] F.J. Martínez-Ruiz, F.J. Blas, A. Moreno-Ventas, J-M-Míguez and L. Macdowell, Phys. Chem. Chem. Phys. **19**, 12296–12309 (2017).
[32] http://chem-siepmann.oit.umn.edu/siepmann/trappe/index.html, (retrieved November, 2019) .
[33] E.A. Müller and G. Jackson, Annu. Rev. Chem. Biomol. Eng. **5**, 405–427 (2014).
[34] P. Orea and G. Odriozola, J. Chem. Phys. **138**, 214105 (2013).
[35] L. Padilla and A. Benavides, J. Chem. Phys. **147**, 034502 (2017).
[36] A. Torres-Carbajal, V.M. Trejos and L. Nicasio-Collazo, J. Chem. Phys. **149**, 144501 (2018).
[37] M.A. Sandoval-Puentes, A. Torres-Carbajal, A.B. Zavala-Martínez, R. Castañeda-Priego and J.M. Méndez-Alcaraz, Journal of Physics: Condensed Matter **34** (16), 164001 (2022).
[38] R. Perdomo-Pérez, J. Martínez-Rivera, N.C. Palmero-Cruz, M.A. Sandoval-Puentes, J.A. Gallegos, E. Lázaro-Lázaro, N.E. Valadez-Pérez, A. Torres-Carbajal and R. Castañeda-Priego, Journal of Physics: Condensed Matter **34** (14), 144005 (2022).
[39] I. Zerón, C. Vega and A. Benavides, Mol. Phys. **116**, 3355–3365 (2018).
[40] D. van der Spoel, E. Lindahl, B. Hess, G. Groenhof, A.E. Mark and H.J. Berendsen, J. Comput. Chem. **26** (16), 1701–1718 (2005).
[41] S. Plimpton, J. Comput. Phys. **117**, 1–19 (1995).
[42] J.P. Hansen and I.R. McDonald, *Theory of Simple Liquids, 3rd Edition* (Academic Press, London, 2013).
[43] W.G. Chapman, K.E. Gubbins, G. Jackson and M. Radosz, Fluid Phase Equil. **52**, 31–38 (1989).
[44] W.G. Chapman, K.E. Gubbins, G. Jackson and M. Radosz, Ind. Eng. Chem. Res. **29** (8), 1709–1721 (1990).
[45] M.S. Wertheim, J. Stat. Phys. **35**, 19–34 (1984).
[46] M.S. Wertheim, J. Stat. Phys. **42**, 459–476 (1986).
[47] M.S. Wertheim, J. Stat. Phys. **42** (3–4), 477–492 (1986).
[48] M.S. Wertheim, J. Chem. Phys. **87** (12), 7323–7331 (1987).
[49] S. Nosé, Mol. Phys. **52**, 255–268 (1984).
[50] W.G. Hoover, Phys. Rev. A **31**, 1695 (1985).
[51] A. Gil-Villegas, A. Galindo, P.J. Whitehead, S.J. Mills, G. Jackson and A.N. Burgess, J. Chem. Phys. **106**, 4168–4186 (1997).
[52] A. Galindo, L.A. Davies, A. Gil-Villegas and G. Jackson, Mol. Phys. **93**, 241–252 (1998).
[53] F.J. Martínez-Ruiz, F.J. Blas, B. Mendiboure and A.I. Moreno-Ventas Bravo, J. Chem. Phys. **141**, 184701/1–17 (2014).
[54] J.S. Rowlinson and F.L. Swinton, *Liquids and Liquid Mixtures* (Butterworth, London, 1982).
[55] H.W. Xiang, *The Corresponding-States Principle and Its Practice Thermodynamic.*

Transport and Surface Properties of Fluids (Elsevier, Amsterdam, 2005).
[56] J.S. Rowlinson and B. Widom, *Molecular Theory of Capillarity* (Claredon Press, London, 1982).
[57] E.A. Guggenheim, J. Chem. Phys. **13**, 253–261 (1945).
[58] B. Widom, J. Chem. Phys. **43**, 3892 (1965).
[59] E. Feria, J. Algaba, J.M. Míguez, A. Mejía, P. Gómez-Álvarez and F.J. Blas, Phys. Chem. Chem. Phys. **22**, 4974–4983 (2020).
[60] L.G. MacDowell and F.J. Blas, J. Chem. Phys. **131**, 074705/1–10 (2009).
[61] F.J. Blas, L.G. MacDowell, E.D. Miguel and G. Jackson, J. Chem. Phys. **129**, 144703 (2008).
[62] C. Vega and E.D. Miguel, J. Chem. Phys. **126**, 154707 (2007).
[63] P.G. de Gennes, F. Brochard-Wyart and D. Quere, *Capillarity and Wetting Phenomena* (Springer, New York, 2004).